JETP Letters, Vol. 71, No. 2, 2000, pp. 92–96. From Pis'ma v Zhurnal Éksperimental'noĭ i Teoreticheskoĭ Fiziki, Vol. 71, No. 2, 2000, pp. 132–138.

CONDENSED MATTER

c-Axis Penetration Depth in $Bi_2Sr_2CaCu_2O_{8+\delta}$ Single Crystals Measured by *ac*-Susceptibility and Cavity Perturbation Technique[1]

D. V. Shovkun, M. R. Trunin, A. A. Zhukov, Yu. A. Nefyodov, N. Bontemps*, H. Enríquez*, A. Buzdin, M. Daumens**, and T. Tamegai*****

Institute of Solid State Physics, Russian Academy of Sciences, Chernogolovka, Moscow oblast, 142432 Russia

** Laboratoire de Physique de la Matière Condensée, Ecole Normale Supérieure, 75231 Paris, France*

*** Laboratoire de Physique Théorique, Université Bordeaux I, 33405 Talence Cedex, France*

**** Department of Applied Physics, The University of Tokyo, Hongo, Bunky-ku, 113-8656 Japan*

Received December 24, 1999

Abstract—The *c*-axis penetration depth $\Delta\lambda_c$ in $Bi_2Sr_2CaCu_2O_{8+\delta}$ (BSCCO) single crystals as a function of temperature has been determined using two techniques, namely, measurements of the *ac*-susceptibility at a frequency of 100 kHz and the surface impedance at 9.4 GHz. Both techniques yield an almost linear function $\Delta\lambda_c(T) \propto T$ in the temperature range $T < 0.5T_c$. Electrodynamic analysis of the impedance anisotropy has allowed us to estimate $\lambda_c(0) \approx 50$ μm in BSCCO crystals overdoped with oxygen ($T_c \approx 84$ K) and $\lambda_c(0) \approx 150$ μm at the optimal doping level ($T_c \approx 90$ K). *© 2000 MAIK "Nauka/Interperiodica".*

PACS numbers: 74.72.Hs; 74.25.Ha

Cuprate high-temperature superconductors (HTS) are layered anisotropic materials. Therefore the electrodynamic problem of the magnetic field penetration depth in HTS in the low-field limit is characterized by two length parameters, namely, λ_{ab} controlled by screening currents running in the CuO_2 planes (in-plane penetration depth) and λ_c due to currents running in the direction perpendicular to these planes (out-of-plane or *c*-axis penetration depth). The temperature dependence of the penetration depth in HTS is largely determined by the superconductivity mechanism. It is known (see, e.g., [1] and references therein) that $\Delta\lambda_{ab}(T) \propto T$ in the range $T < T_c/3$ in high-quality HTS samples at the optimal level of doping, and this observation has found the most simple interpretation in the *d*-wave model of the high-frequency response in HTS [2]. Measurements of $\Delta\lambda_c(T)$ are quoted less frequently than those of $\Delta\lambda_{ab}(T)$. Most of such data published were derived from microwave measurements of the surface impedance of HTS crystals [3–11]. There is no consensus in literature about $\Delta\lambda_c(T)$ at low temperatures. Even in reports on low-temperature properties of high-quality YBCO crystals, which are the most studied objects, one can find both linear, $\Delta\lambda_c(T) \propto T$ [4, 9], and quadratic dependences [11] in the range $T < T_c/3$. In BSCCO materials, the shape of $\Delta\lambda_c(T)$ depends on the level of oxygen doping: in samples with maximal $T_c \simeq 90$ K $\Delta\lambda_c(T) \propto T$ at low temperatures [7, 8]; at higher oxygen contents (overdoped samples) T_c is lower and the linear function $\Delta\lambda_c(T)$ transforms to a quadratic one [8]. The common feature of all microwave experiments is that the change in the ratio $\Delta\lambda_c(T)/\lambda_c(0)$ is smaller than in $\Delta\lambda_{ab}(T)/\lambda_{ab}(0)$ because in all HTS $\lambda_c(0) \gg \lambda_{ab}(0)$. The length $\lambda_c(0)$ is especially large in BSCCO crystals, $\lambda_c(0) > 10$ μm and, according to some estimates, it ranges up to ~500 μm. The large spread of $\lambda_c(0)$ is caused by two factors, namely, the poor accuracy of the techniques used in determination of $\lambda_c(0)$ and effects of local and extended defects in tested samples, whose range is of the order of 1 mm and comparable to both λ_c and total sample dimensions.

Recently, we suggested [12] a new technique for determination of $\lambda_c(0)$ based on the measurements of the surface barrier field $H_J(T) \propto 1/\lambda_c(T)$ at which Josephson vortices penetrate into the sample. The field H_J corresponds to the onset of microwave absorption in the locked state of BSCCO single crystals. This paper suggests an alternative technique based on comparison between microwave measurements of BSCCO crystals aligned differently with respect to ac magnetic field and a numerical solution of the electrodynamic problem of the magnetic field distribution in an anisotropic plate at an arbitrary temperature. Moreover, since $\lambda_c(0)$ in BSCCO single crystals is relatively large, we managed to determine $\lambda_c(T)$ from the temperature dependences of *ac*-susceptibility and compare these measurements to results of microwave experiments.

[1] This article was submitted by the authors in English.

Single crystals of BSCCO were grown by the floating-zone method [13] and shaped as rectangular platelets. This paper presents measurements of two BSCCO samples with various levels of oxygen doping. The first sample (#1), characterized by a higher critical temperature, $T_c \approx 90$ K (optimally doped), has dimensions $a \times b \times c \simeq 1.5 \times 1.5 \times 0.1$ mm^3 ($a \approx b$). The second (#2, $a \times b \times c \simeq 0.8 \times 1.8 \times 0.03$ mm^3) is slightly overdoped ($T_c \approx 84$ K).

When measuring the *ac*-susceptibility $\chi = \chi' - i\chi''$, we placed a sample inside one of two identical induction coils. The coils were connected to one another, and the out-of-phase and in-phase components of the imbalance signal were measured at a frequency of 10^5 Hz. These components are proportional to the real and imaginary parts of the sample magnetic moment M, respectively: $M = \chi v H_0$, where v is the sample volume and H_0 is the ac magnetic field amplitude, which was within 0.1 Oe in our experiments.

Figure 1 shows temperature dependences $\chi'(T)/|\chi'(0)|$ in sample #1 for three different sample alignments with respect to the ac magnetic field: the transverse (T) orientation, $\mathbf{H}_\omega \parallel \mathbf{c}$, (the inset on the left of Fig. 1), when the screening current flows in the *ab*-plane (full circles); in the longitudinal (L) orientation, $\mathbf{H}_\omega$, (the inset on the right of Fig. 1, $\mathbf{H}_\omega \perp \mathbf{c}$ is parallel to the *b*-edge of the crystal), when currents running in the directions of both CuO_2 planes and the *c*-axis are present (up triangles); in the L-orientation, $\mathbf{H}_\omega \perp \mathbf{c}$, whose difference from the previous configuration is that the sample is turned around the *c*-axis through 90° (down triangles). Figure 1 clearly shows that at $T < T_c \chi'_{ab}(T)$ is notably smaller in the T-orientation than $\chi'_{ab+c}(T)$ in the L-orientation (the subscripts of χ' denote the direction of the screening current). The coincidence of $\chi'_{ab+c}(T)$ curves at $\mathbf{H}_\omega \perp \mathbf{c}$ and the small width of the superconducting transition at $\mathbf{H}_\omega \parallel \mathbf{c}$ ($\Delta T_c < 1$ K) indicate that the quality of tested sample #1 is fairly high. This is supported by precision measurements of surface impedance $Z_s(T) = R_s(T) + iX_s(T)$ of sample #1 at frequency $f = 9.4$ GHz in the T-orientation, which are plotted in Fig. 2. The measurement technique was described in detail elsewhere [1]. It applies to both surface impedance components $R_s(T)$ and $X_s(T)$:

$$R_s = \Gamma_s \Delta(1/Q), \quad X_s = -2\Gamma_s \delta f/f. \qquad (1)$$

Here, $\Gamma_s = \omega\mu_0 \int_V H_\omega^2 dV / [\int_S H_s^2 dS]$ is the sample geometrical factor ($\omega = 2\pi f$, $\mu_0 = 4\pi \times 10^{-7}$ H/m, V is the volume of the cavity, H_ω is the magnetic field generated in the cavity, S is the total sample surface area, and H_s is the tangential component of the microwave magnetic field on the sample surface); $\Delta(1/Q)$ is the difference between the values $1/Q$ of the cavity with the sample inside and empty cavity; and δf is the frequency shift relative to that

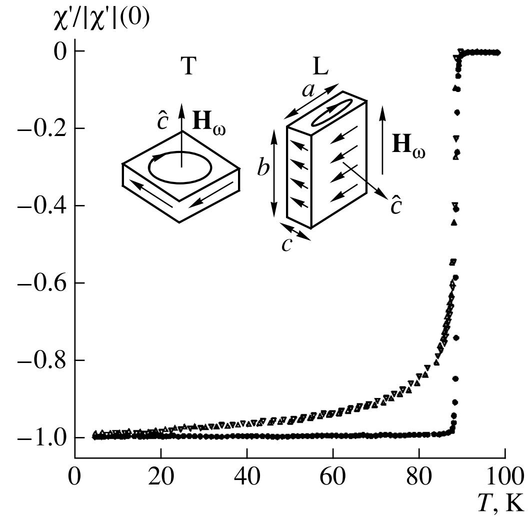

Fig. 1. Curves of the *ac*-susceptibility of sample #1 versus temperature in different orientation with respect to ac magnetic field: $\mathbf{H}_\omega \parallel \mathbf{c}$ (full circles); $\mathbf{H}_\omega \perp \mathbf{c}$, $\mathbf{H}_\omega$ is parallel to the *b*-edge of the crystal (up triangles); $\mathbf{H}_\omega \perp \mathbf{c}$, $\mathbf{H}_\omega$, is parallel to the *a*-edge of the crystal (down triangles). Left-hand inset: transverse (T) orientation, $\mathbf{H}_\omega \parallel \mathbf{c}$, the arrows on the surfaces show directions of the screening current. Right-hand inset: Longitudinal (L) orientation, $\mathbf{H}_\omega \perp \mathbf{c}$.

which would be measured for a sample with perfect screening, i.e., no penetration of the microwave fields. In the experiment, we measure the difference $\Delta f(T)$ between resonant frequency shifts with temperature of the loaded and empty cavity, which is equal to $\Delta f(T) = \delta f(T) + f_0$, where f_0 is a constant.[2] The constant f_0 includes both the perfect-conductor shift and the uncontrolled contribution caused by opening and closing the cavity. In HTS single crystals, the constant f_0 can be directly derived from measurements of the surface impedance in the normal state; in particular, in the T-orientation, f_0 can be derived from the condition that the real and imaginary parts of the impedance should be equal above T_c (normal skin-effect). In Fig. 2, $R_s(T) = X_s(T)$ at $T \geq T_c$, and its temperature dependence is adequately described by the expression $2R_s^2(T)/\omega\mu_0 = \rho(T) = \rho_0 + bT$ with $\rho_0 \approx 13$ μΩ cm and $b \approx 0.3$ μΩ cm/K. Given $R_s(T_c) = \sqrt{\omega\mu_0\rho(T_c)/2} \approx 0.12\ \Omega$, we obtain the resistivity $\rho(T_c) \approx 40$ μΩ cm. The insets to Fig. 2 show $R_s(T)$ and $\lambda(T) = X_s(T)/\omega\mu_0$ for $T < 0.7\, T_c$ plotted on a linear scale. The extrapolation of the low-temperature sections of these curves to $T = 0$ yields estimates of $\lambda_{ab}(0) \approx 2600$ Å and the residual surface resistance $R_{res} \approx 0.5\ m\Omega$. R_{res} is due to various defects in the surface layer of the superconductor and it is generally accepted that the lower the R_{res}, the better the sample quality. The above mentioned

[2] We note that $\delta f(T)$ includes the frequency shift due to the sample thermal expansion, which is essential for $T > 0.7T_c$ in the T-orientation [1].

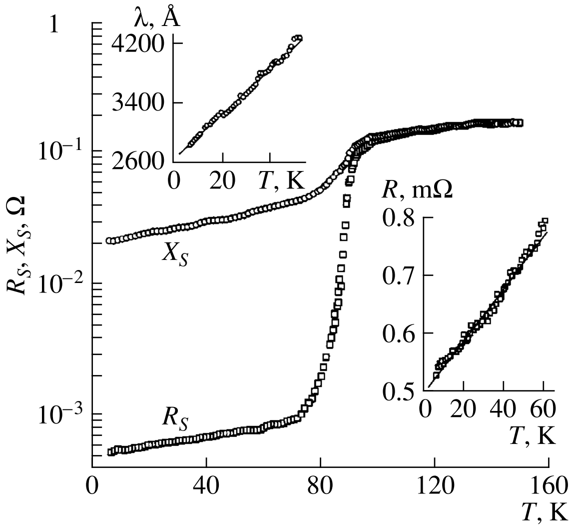

Fig. 2. Surface resistance $R_s(T)$ and reactance $X_s(T)$ in *ab*-plane (T-orientation) of sample #1 at 9.4 GHz. The insets show linear plots of $\lambda(T)$ and $R_s(T)$ at low temperatures.

parameters of sample #1 indicate that its quality is fairly high. In the T-orientation, linear functions $R_s(T)$ and $\Delta\lambda_{ab}(T)$ in the low-temperature range were previously observed in optimally doped BSCCO crystals at a frequency of about 10 GHz [7, 8, 14]. In the slightly overdoped sample #2 we also observed $\Delta\lambda_{ab}(T)$, $\Delta R_s(T) \propto T$ at low temperature, moreover, the measurement $R_{res} \approx$ 120 μΩ is, to the best of our knowledge, the lowest value ever obtained in BSCCO single crystals.

In both superconducting and normal states of HTS, the relation between electric field and current density is local: $j = \hat{\sigma} E$, where the conductivity $\hat{\sigma}$ is a tensor characterized by components σ_{ab} and σ_c. In the normal state, ac field penetrates in the direction of the *c*-axis through the skin depth $\delta_{ab} = \sqrt{2/\omega\mu_0\sigma_{ab}}$ and in the CuO_2 plane through $\delta_c = \sqrt{2/\omega\mu_0\sigma_c}$. In the superconducting state, all parameters δ_{ab}, δ_c, $\sigma_{ab} = \sigma'_{ab} - i\sigma''_{ab}$, and $\sigma_c = \sigma'_c - i\sigma''_c$ are complex. In the temperature range $T < T_c$, if $\sigma' \ll \sigma''$, the field penetration depths are given by the formulas $\lambda_{ab} = \sqrt{1/\omega\mu_0\sigma''_{ab}}$, $\lambda_c = \sqrt{1/\omega\mu_0\sigma''_c}$. In the close neighborhood of T_c, if $\sigma' \gtrsim \sigma''$, the decay of magnetic field in the superconductor is characterized by the functions $\mathrm{Re}(\delta_{ab})$ and $\mathrm{Re}(\delta_c)$, which turn to δ_{ab} and δ_c, respectively, at $T \geq T_c$.

In the L-orientation of BSCCO single crystals at $T < 0.9T_c$, the penetration depth is smaller than characteristic sample dimensions. If we neglect the anisotropy in the *ab*-plane and the contribution from *ac*-faces (see the inset to Fig. 1), which is a factor ~ c/b smaller than that of the *ab*-surfaces, the effective impedance Z_s^{ab+c} in the L-orientation can be expressed in terms of Z_s^{ab} and Z_s^c averaged over the surface area [1, 5] (the superscripts of Z_s denote the direction of the screening current). Thus, given measurements of $\Delta\lambda_{ab}(T) = \Delta X_s^{ab}(T)/\omega\mu_0$ in the T-orientation and of the effective value $\Delta\lambda_{ab+c}(T) = \Delta X_s^{ab+c}(T)/\omega\mu_0$ in the L-orientation, we obtain

$$\Delta\lambda_c = [(a+c)\Delta\lambda_{ab+c} - a\Delta\lambda_{ab}]/c. \qquad (2)$$

This technique for determination of $\Delta\lambda_c(T)$ was used in microwave experiments [3–9] at low temperatures, $T < T_c$. Even so, this cannot be applied to the range of higher temperatures because the size effect plays an important role. Really, at $T > 0.9T_c$ the lengths λ_c and δ_c are comparable to the sample dimensions. In order to analyze our measurements in both superconducting and normal states of BSCCO, we used formulas [15] for field distributions in an anisotropic long strip ($b \gg a, c$) in the L-orientation. These formulas neglect the effect of *ac*-faces of the crystal, but take account of the size effect. In addition, in a sample shaped as a long strip, there is a simple relation between its surface impedance components and *ac*-susceptibility, which is expressed in terms of parameter μ introduced in [15]:

$$\Delta(1/Q) - 2i\delta f/f = i\gamma\mu v/V, \quad \chi = -1+\mu, \qquad (3)$$

where $\gamma = VH_0^2/[\int_V H_\omega^2 dV] = 10.6$ is a constant characterizing our cavity [1]. At an arbitrary temperature, the complex parameter $\mu = \mu' - i\mu''$ is controlled by the components $\sigma_{ab}(T)$ and $\sigma_c(T)$ of the conductivity tensor:

$$\mu = \frac{8}{\pi^2}\sum_n \frac{1}{n^2}\left\{\frac{\tan(\alpha_n)}{\alpha_n} + \frac{\tan(\beta_n)}{\beta_n}\right\}, \qquad (4)$$

where the sum is performed over odd integers $n > 0$, and

$$\alpha_n^2 = -\frac{a^2}{\delta_c^2}\left(\frac{i}{2} + \frac{\pi^2}{4}\frac{\delta_{ab}^2}{c^2}n^2\right),$$

$$\beta_n^2 = -\frac{c^2}{\delta_{ab}^2}\left(\frac{i}{2} + \frac{\pi^2}{4}\frac{\delta_c^2}{a^2}n^2\right).$$

In the superconducting state at $T < 0.9T_c$ we find that $\lambda_{ab} \ll c$ and $\lambda_c \ll a$. In this case, we derive from (4) a simple expression for the real part of μ:

$$\mu' = 1 + \chi' = \frac{2\lambda_c}{a} + \frac{2\lambda_{ab}}{c}. \qquad (5)$$

One can easily check up in the range of low temperatures, the change in $\Delta\lambda_c(T)$ prescribed by (5) is identical to (2). Figure 3 shows measurements of $\Delta\lambda_c(T)$ in sample

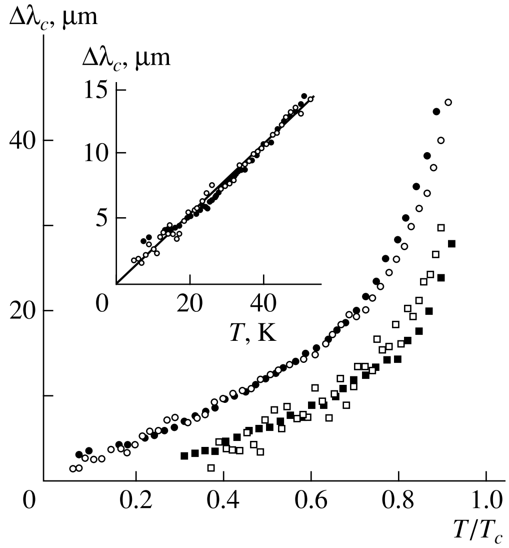

Fig. 3. Temperature dependences $\Delta\lambda_c$ in samples #1 (circles) and #2 (squares) at $T < 0.9\,T_c$. Open symbols plot low-frequency measurements, full symbols show microwave data. The inset shows low temperature sections of the $\Delta\lambda_c$ curves in sample #1.

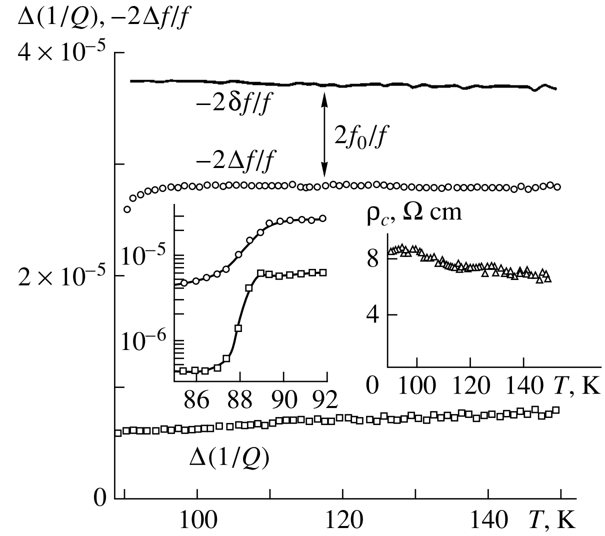

Fig. 4. Temperature dependences of $\Delta(1/Q)$ (open squares) and $-2\Delta f/f$ (open circles) in the L-orientation of sample #1 at $T > T_c$. Solid line shows the function $-2\delta f(T)/f$ deriving from (3). Left-hand inset: $\Delta(1/Q)$ and $-2\Delta f/f$ as functions of temperature in the neighborhood of T_c. Right-hand inset: $\rho_c(T)$ in sample #1 (triangles).

#1 (circles) and sample #2 (squares) at $T < 0.9T_c$. The open symbols plot low-frequency measurements obtained in accordance with (5), the full symbols plot microwave measurements processed by (2). Agreement between measurements of sample #2 (lower curve) is fairly good, but in fitting together experimental data from sample #1 (upper curve) we had to divide by a factor of 1.8 all $\Delta\lambda_c(T)$ derived from measurements of *ac*-susceptibility using (5). The cause of the difference between $\Delta\lambda_c(T)$ measured in sample #1 at different frequencies is not quite clear. We rule out a systematic experimental error that could be caused by misalignment of the sample with respect to the ac magnetic field because the curves of $\Delta\lambda_c(T)$ were accurately reproduced when square sample #1 was turned through an angle of 90° in the L-orientation. It seems more plausible that (2) and (5), which neglect the contribution of *ac*-faces, yield inaccurate results concerning sample #1: its *ac*-faces, which have a notable area (sample #1 is thick), can lose a lot of defects (for example hose of the capacitive type), and the latter can affect the character of field penetration as a function of frequency.

The curves of $\Delta\lambda_c(T)$ at $T < 0.5\,T_c$ plotted in Fig. 3 are almost linear $\Delta\lambda_c(T) \propto T$. The inset to Fig. 3 shows the low-temperature section of the curve of $\Delta\lambda_c(T)$ in sample #1. Its slope is 0.3 μm/K and equals that from [8]. Note also that changes in $\Delta\lambda_c(T)$ are smaller in the oxygen-overdoped sample #2 than in sample #1.

We can estimate $\lambda_c(0)$ by substituting in (1) $\delta f(0)$ obtained by comparing $\Delta(1/Q)$ and $\Delta f = \delta f - f_0$ measurements taken in the T- and L-orientations to numerical calculations by (3) and (4), which take into account the size effect in the high-frequency response of an anisotropic crystal. The procedure of comparison for sample #1 is illustrated by Fig. 4. Unlike the case of the T-orientation, the measured temperature dependence of $\Delta(1/Q)$ in the L-orientation deviates from $(-2\Delta f/f)$ owing to the size effect. Using the measurements of $R_s = \sqrt{\omega\mu_0/2\sigma_{ab}}$ at $T > T_c$ in the T-orientation (Fig. 2) for determination of $\sigma_{ab}(T)$, alongside the data on $\Delta(1/Q)$ in the L-orientation (open squares in Fig. 4), from (3) and (4) we obtain the curve of $\rho_c(T) = 1/\sigma_c(T)$ shown in the right-hand inset to Fig. 4. Further, using the functions $\sigma_c(T)$ and $\sigma_{ab}(T)$, we calculate $(-2\delta f/f)$ versus temperature for $T > T_c$, which is plotted by the solid line in Fig. 4. This line is approximately parallel to the experimental curve of $-2\Delta f/f$ in the L-orientation (open circles in Fig. 4). The difference $-2(\delta f - \Delta f)/f$ yields the additive constant f_0. Given f_0 and $\Delta f(T)$ measured in the range $T < T_c$, we also obtain $\delta f(T)$ in the superconducting state in the L-orientation. As a result, with due account of $\lambda_{ab}(T)$ (the inset to Fig. 2), we derive from (3) and (5) $\lambda_c(0)$, which equals approximately 150 μm in sample #1. A similar procedure performed with sample #2 yields $\lambda_c(0) \approx 50$ μm, which is in agreement with our measurements of overdoped BSCCO obtained using a different technique [12]. We also estimated $\lambda_c(0)$ on the base of absolute measurements of the susceptibility $\chi_c'(0)$ from (5), and we obtained $\lambda_c(0) \approx 210$ μm for sample #1 and $\lambda_c(0) \approx 70$ μm for sample #2. These results are in reasonable agreement with our microwave measurements if we take into consideration the fact that the accuracy of λ_c measurements is rather poor and the error can be up to 30%.

In conclusion, we have used the *ac*-susceptibility and cavity perturbation techniques in studying anisotropic high frequency properties of BSCCO single crystals. We have observed almost linear dependences $\Delta\lambda_c(T) \propto T$, which are in fair agreement with both experimental [7, 8, 12] and theoretical [16] results by other researchers. We have also investigated a new technique for determination of $\lambda_c(0)$, which is a factor of three higher in the optimally doped BSCCO sample than in the overdoped crystal. The ratio between the slopes of curves of $\Delta\lambda_c(T)$ in the range $T \ll T_c$ is the same. These facts could be put down to dependences of $\lambda_c(0)$ and $\Delta\lambda_c(T)$ on the oxygen content in these samples. At the same time, we cannot rule out the influence of defects in the samples on $\lambda_c(0)$, even though their quality in the *ab*-plane is fairly high, according to our experiments. In order to draw ultimate conclusions concerning the nature of the transport properties along the *c*-axis in BSCCO single crystals, studies of more samples with various oxygen contents are needed.

ACKNOWLEDGMENTS

We would like to thank V.F. Gantmakher for his helpful discussions. This research was supported by grant no. 4985 of the CNRS-RAS cooperation. The work at ISSP was also supported by the Russian Foundation for Basic Research, grants nos. 97-02-16836 and 98-02-16636 and the Scientific Council on Superconductivity, project no. 96060.

REFERENCES

1. M. R. Trunin, Phys.-Usp. **41**, 843 (1998); J. Supercond. **11**, 381 (1998).
2. D. J. Scalapino, Phys. Rep. **250**, 329 (1995).
3. T. Shibauchi, H. Kitano, K. Uchinokura, *et al.*, Phys. Rev. Lett. **72**, 2263 (1994).
4. J. Mao, D. H. Wu, J. L. Peng, *et al.*, Phys. Rev. B **51**, 3316 (1995).
5. H. Kitano, T. Shibauchi, K. Uchinokura, *et al.*, Phys. Rev. B **51**, 1401 (1995).
6. D. A. Bonn, S. Kamal, K. Zhang, *et al.*, J. Phys. Chem. Solids **56**, 1941 (1995).
7. T. Jacobs, S. Sridhar, Q. Li, *et al.*, Phys. Rev. Lett. **75**, 4516 (1995).
8. T. Shibauchi, N. Katase, T. Tamegai, *et al.*, Physica C **264**, 227 (1996).
9. H. Srikanth, Z. Zhai, S. Sridhar, *et al.*, J. Phys. Chem. Solids **59**, 2105 (1998).
10. H. Kitano, T. Hanaguri, and A. Maeda, Phys. Rev. B **57**, 10946 (1998).
11. A. Hosseini, S. Kamal, D. A. Bonn, *et al.*, Phys. Rev. Lett. **81**, 1298 (1998).
12. H. Enríquez, N. Bontemps, A. A. Zhukov, *et al.*, submitted to Phys. Rev. B.
13. S. Ooi, T. Shibauchi, and T. Tamegai, Physica C **302**, 339 (1998).
14. S.-F. Lee, D. C. Morgan, R. J. Ormeno, *et al.*, Phys. Rev. Lett. **77**, 735 (1996).
15. C. E. Gough and N. J. Exon, Phys. Rev. B **50**, 488 (1994).
16. R. A. Klemm and S. H. Liu, Phys. Rev. Lett. **74**, 2343 (1995); T. Xiang and J. M. Wheatley, Phys. Rev. Lett. **76**, 134 (1996); R. J. Radtke, V. N. Kostur, and K. Levin, Phys. Rev. B **53**, R522 (1996).